Plasma Treatment of the Large-Area Polymer Substrates for the Enhanced Adhesion of UV-Digital Printing

Michal Fleischer , Zlata Kelar Tučeková * , Oleksandr Galmiz , Eva Baťková , Tomáš Plšek , Tatiana Kolářová , Dušan Kováčik , Jakub Kelar

Posted Date: 2 February 2024

doi: 10.20944/preprints202402.0178.v1

Keywords: UV-digital printing; transparent polymers; low-temperature plasma; surface functionalization; ink adhesion.

 doi:10.20944/preprints202402.0178.v1

Article

Plasma Treatment of the Large-Area Polymer Substrates for the Enhanced Adhesion of UV-Digital Printing

Michal Fleischer, Zlata Kelar Tučeková *, Oleksandr Galmiz, Eva Baťková, Tomáš Plšek, Tatiana Kolářová, Dušan Kováčik and Jakub Kelar

Department of Plasma Physics and Technology, CEPLANT—R&D Centre for Plasma and Nanotechnology Surface Modifications, Faculty of Science, Masaryk University, Kotlářská 2, 611 37 Brno, Czech Republic; michal.fleischer@mail.muni.cz (M.F.); o.galmiz@mail.muni.cz (O.G.); 484056@mail.muni.cz (E.K.); 461281@mail.muni.cz (T.P.); t.zahoranova@yahoo.com (T.K.); dusan.kovacik@mail.muni.cz (D.K.); jakub.kelar@mail.muni.cz (J.K.)

* Correspondence: zlata.tucekova@mail.muni.cz

Abstract: UV-digital printing belongs to the commonly used method for custom large-area substrate decoration. Despite low surface energy and adhesion, transparent polymer materials, such as polymethylmethacrylate (PMMA) and polycarbonate (PC), represent an ideal substrate for such purposes. The diffuse coplanar surface barrier discharge (DCSBD) in a novel compact configuration was used for substrate activation to improve ink adhesion to the polymer surface. This industrially applicable version of DCSBD was prepared, tested, and successfully implemented for the UV-digital printing process. Furthermore, wettability and surface free energy measurement, X-ray photoelectron spectroscopy, atomic force and scanning electron microscopy evaluated the surface chemistry and morphology changes. The changes in adhesion of the surface and of ink were analyzed by a peel-force and a crosscut test, respectively. A short plasma treatment (1-5 s) enhanced the substrate's properties of PMMA and PC while providing the pre-treatment suitable for further in-line UV-digital printing. Furthermore, we did not observe damage or significant change of roughness affecting the substrate's initial transparency.

Keywords: UV-digital printing; transparent polymers; low-temperature plasma; surface functionalization; ink adhesion.

1. Introduction

Plasmas operating at atmospheric pressure have found widespread commercial use as a tool for polymer pre-treatment [1,2]. Activating the polymer surface improves surface free energy, adhesive bonding strength, paint adhesion and dye uptake [3]. Meanwhile, an increase in the material surface roughness can benefit the bonding and coating of the material surface [4]. Atmospheric low-temperature plasmas (LTPs) are an interesting alternative to other pre-treatment methods (e.g., low-pressure plasmas [5,6], wet chemical or radiation treatment [3,7]) because of their relatively low costs, in-line process capabilities, and personal and environmental safety requirements [8–11].

One of the most recent industrial applications of LTP is large-format UV-digital printing [12–14]. The stability of such printing depends on the choice of substrate materials and the printed color pattern. Commonly used polymeric materials have a smooth surface and low surface energy, which often (but not inevitably) causes insufficient adhesion of inks used for UV-digital printing [14–16]. The adhesion of the printed color pattern, or its abrasion resistance, then affects the final product's usage and positioning, or the printed substrate's impact, depending on climatic conditions (e.g., outdoor conditions, humidity, and temperature).

This paper used the LTP treatment by special diffuse coplanar surface barrier discharge (DCSBD) [9] to modify the surface of PC and PMMA substrates, often considered glass substitutes in UV-digital printing. The end-user of UV-digital printers requires a substantial increase in the

 doi:10.20944/preprints202402.0178.v1

adhesion and standardization of the printed layer quality on polymer substrates from different manufacturers [16]. Thus, process variables (plasma reactor configuration, treatment time, and treatment distance) were identified and used for experimental tests. The polymer surface's chemical composition and morphology changes are studied. The adhesion properties of the activated samples are determined by peel-force measurement and a standard crosscut ink adhesion test after UV-digital printing.

2. Materials and Methods

2.1. Materials

The industrial-grade Polycarbonate and Poly(methyl methacrylate) substrates provided by Effetec s.r.o. (Čelechovice na Hané, Czech Republic) were used for experiments. Samples were delivered in the form of boards with dimensions of 15×10 cm^2 with an approximate thickness of 3 mm. For different experiments, samples have been cut into smaller pieces with dimensions of 1.5×10 cm^2. Protective foil has been removed prior to plasma treatment without any additional cleaning of the sample surface.

2.2. Plasma Treatment

The LTP treatment of polymeric substrates proceeded at different distances from the sample (225 um, 300 um and 450 um) in dynamic mode (i.e., plasma source moving above the substrate). The exposure time varied in the range of 1-5 s. The short exposure times were ensured by changing the speed of plasma source movement, and prolonged treatment resulted from repeated 5 s exposure. Plasma-treated samples were stored for up to 3 days in a desiccator cabinet at 23°C and humidity of 40% to ensure the ageing at controlled conditions.

The plasma was generated by two DBD versions, DCSBD and half-DCSBD (HDCSBD). The DCSBD generates a macroscopically homogeneous LTP with an input power of 400 W at ~15 kHz [17]. The active-discharge area is ~8×20 cm^2. Figure 1a) shows the simplified scheme of the DCSBD plasma source. The more detailed technical specifications of DCSBD are listed in [9].

The HDCSBD is a unique approach to the DCSBD configuration manufactured by KYOCERA Inc. (Kyoto, Japan) but designed and protected by Masaryk University. The cooling by flowing dielectric oil is replaced with an industrial aluminum heat sink and a fan with adjustable airflow. The scheme of HDCSBD is shown in Figure 1b. Plasma generated by HDCSBD has comparable properties to plasma created by DCSBD. The input power is 200 W at ~20 kHz, and the active discharge area is ~8×10 cm^2. These parameters served to design the prototype of the printing device with the implemented plasma technology photographed in Figure 2.

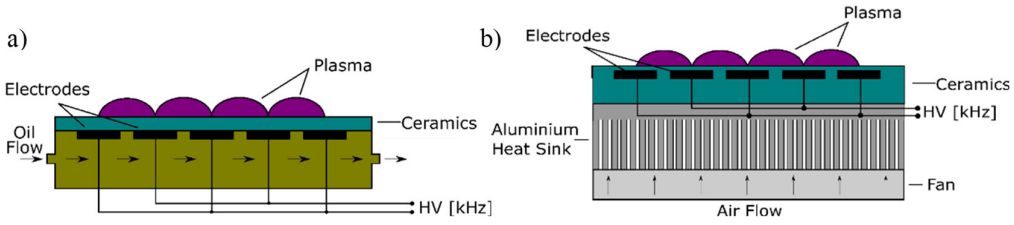

Figure 1. The simplified scheme of a) DCSBD and b) HDCSBD plasma technology.

 doi:10.20944/preprints202402.0178.v1

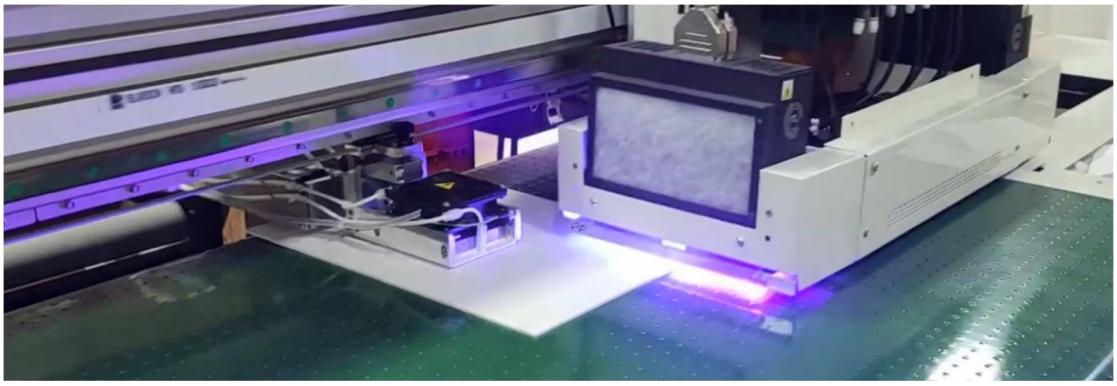

Figure 2. The photograph of the UV-digital printer prototype with implemented HDCSBD technology during UV-LED curing (legally protected by outcomes listed in Chapter 5).

2.3. Analytical Methods for Plasma Treatment Evaluation

2.3.1. Wettability Measurements

To calculate dispersive and polar components of surface free energy (SFE), the droplets formed on the substrate were evaluated by the Owens-Wendt regression model [18] using three liquid method (deionized water, diiodomethane and ethylene glycol). An average of 14 droplets of each liquid placed by a micropipette with a constant volume of 1 µl was used to estimate the contact angles. To capture the photos and measure the profile of the droplets, we used See (Surface Energy Evaluation) System analyzer (Advex Instruments, s.r.o., Brno, Czech Republic). The standard error in SFE measurement was approx. 1 mJ/m^2.

2.3.2. Adhesion of Surface

The static material testing machine Texture Analyser TA.XT plusC (Stable Micro Systems, Surrey, United Kingdom) measured the samples' adhesive properties equipped with a load cell of 50 N range. According to the FINAT method no. 1, the adhesion test (a 180° adhesion peel test) was performed on the samples. The loading speed was 10 mm per minute. Preparation of the samples consisted of attaching a special adhesive tape (TQC Sheen, Rotterdam, Netherlands) according to ISO 2409:1999 and ensuring 12 passes over a taped area with a pre-calibrated rolling pin (2kg). For average peel force calculation, the peel test on a length of 90 mm was repeated on at least 5 samples. The whole process was captured by the software Exponent Connect.

2.3.3. Chemical Characterization

The chemical changes on the surface were analyzed by XPS performed by the spectrometer Axis Supra (Kratos Analytical Ltd., Manchester, United Kingdom) under the same conditions as in [10]. The calibration of spectra, further processing and standard fitting were carried out using CASA software (trial version CasaXPS 2.3.16, CASA international nv, Olen, Belgium).

2.3.4. Morphological Characterization

The roughness changes after the treatment were measured using AFM NTEGRA Prima (NT-MDT, Moscow, Russia) in a semi-contact mode using golden-silicon probes AN-NSG10/50 (Applied NanoStructures Inc., Mountain View, CA, USA). The Root Mean Square (RMS) and Average roughness were estimated from 100-400 um^2 with a resolution of 512×512 px^2 and a scanning frequency of up to 1 Hz.

The morphology changes were observed by SEM microscope Mira3 (Tescan, Brno, Czech Republic). The detector of secondary electrons and accelerating voltage of 7-10 kV was used to magnify the surfaces up to 50,000 times. Before measurement, both substrates were coated with 20

 doi:10.20944/preprints202402.0178.v1

nm of the Au/Pd layer by sputter coater Quorum Q150R-ES (Quorum Technologies, Lewes, United Kingdom).

2.3.5. UV-Digital Printing and Ink Adhesion Evaluation

The custom UV LED head (395 nm, 14 W/cm) cured the acrylate-based ink (EFFE811, Effetec s.r.o.) and pattern with 360 × 1200 DPI resolution. Testing set CC3000 (TQC-Sheen, Rotterdam, Netherland) was used to perform crosscut and tape tests according to DIN ISO 2409:2003 to evaluate the ink adhesion right after and 24 hours after UV-digital printing. After the crosscut peel test, the numbers and boundaries of cuts were examined and compared to the untreated substrate. For this standard test, the samples kept their dimensions of 15×10 cm², and patterns of different colors were printed by a prototype of a UV-digital printing machine (Effetec s.r.o) with implemented HDCSBD technology (Figure 2.).

3. Results and Discussion

The authors will present the results of the DCSBD and HDCSBD treatment of transparent polymers in the following chapters. The following results should compare and prove the compatibility of used plasma sources. Furthermore, the authors intended to emphasize the choice of HDCSBD for its implementation in the UV-digital printing process.

3.1. Wettability and Adhesion of LTP-Treated Substrates

The polymers' total surface free energy (SFE), dispersion and polar components were calculated for a better understanding of the wetting changes of plasma-treated substrates. For better comparison, the PMMA and PC substrates were treated at different distances and times by both DCSBD and HDCSBD sources. Figures 3 and 4 show that the total SFE increased after short LTP exposure, implying improved wettability of polymer surfaces.

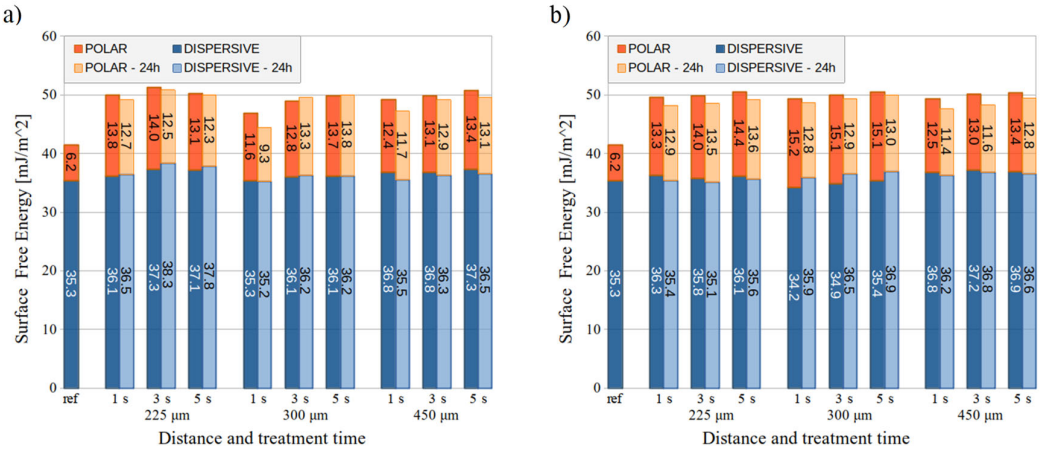

Figure 3. The SFE of PMMA substrates treated by a) the DCSBD and b) the HDCSBD plasma technology.

 doi:10.20944/preprints202402.0178.v1

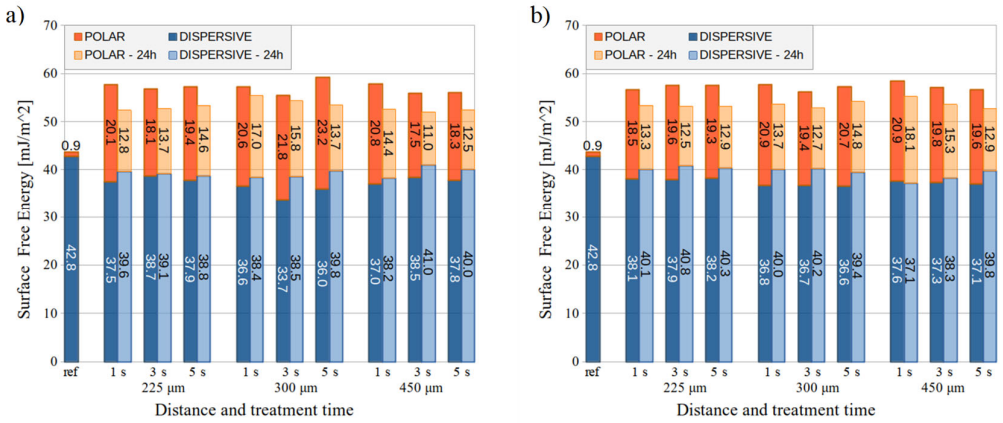

Figure 4. The SFE of PC substrates treated by a) the DCSBD and b) the HDCSBD plasma technology.

Right after the LTP treatment of PMMA, the polar part increase occurred. After 1-day ageing, the polar part slightly decreased but did not return to the initial value. After 3-day ageing (not shown), the achieved polar part remained mostly unchanged within the error. However, the polar part of samples treated for 1 sec by DCSBD and HDCSBD at 300 and 450 um decreased faster during storage.

The dispersion component of PMMA increased slightly by max. 3 mJ/m² after the LTP treatment, except for HDCSBD treatment at 300 um. However, after ageing, the dispersive part of all samples tended to recover towards a slightly increased value compared to the reference value.

In agreement with the study of Homola et al. [19], PMMA from different suppliers and sonicated by isopropanol achieved similar polar values after the 1 s treatment compared with 3 and 9 s air DCSBD exposure at 300 um distance. However, this value (13.1 mJ/m²) was unstable and decreased to 7.7 mJ/m² after 3-day ageing. The dispersive part increased more than in our experiment, contributing to a higher increase in total SFE.

In the case of LTP treatment of PC, the polar component significantly increased by 17-22 mJ/m² while the dispersive part decreased by 4-9 mJ/m². After ageing, the polar component decreased in time while the dispersive part was recovering. However, the SFE components did not achieve initial values even after 3-day ageing (not shown).

In [20], industrial-grade PC was treated by DCSBD at a distance of 300 um. Due to hydrophobic recovery, the gained total SFE decreased by 8-9 mJ/m² after 3 days. In our experiment, the samples treated by DCSBD and HDCSBD at the same distance decreased their total SFE by 5-7 mJ/m² and 5-6 mJ/m² after 3 days, respectively.

Incorporating polar functional groups often explains the increase of polar component on tested polymers. These can be introduced onto the surface due to generating reactive oxygen and nitrogen species (RONS) in air plasma. Moreover, the air humidity and polymer chain characteristics mediate hydroxyl and carboxyl group formation [6,8,10]. The dispersive component reflects the Van der Waals bonds and varies due to the incorporation of nonpolar functional groups (e.g., methyl) and changes in surface morphology. This behaviour is also described in the literature [21] and, in our case, agrees with the XPS results (chapter 3.2).

Surface activation with LTP generally modifies the SFE or surface reactivity through surface oxidation and chemical grafting [4,22,23]. The presented results of SFE measurement imply the formation of polar oxygen-containing functional groups, resulting in increased surface wetting and may provide improvement of adhesion [11,24,25]. Studies have also shown the influence of surface roughness on the coating adhesion after plasma activation. These two complementary effects can increase adhesion phenomena at the interface between the coating and substrate [7,22,25,26]. Nevertheless, as mentioned later (chapters 3.3-3.4), the roughness changes could not dominantly contribute to ink adhesion in the case of both tested polymers.

Preprints.org (www.preprints.org) | NOT PEER-REVIEWED | Posted: 2 February 2024 doi:10.20944/preprints202402.0178.v1

The adhesion changes on PMMA and PC substrates after air DCSBD and HDCSBD treatment at different distances are shown in Figures 5 and 6. The 1 s treatment was excluded from the adhesion evaluation due to many samples and measurements needed right after exposure and after 24-hour ageing. Other reasons were the aforementioned fast ageing of 1 s treated PMMA samples and optimal treatment time evaluated in previous studies [19,20] on similar industrial-grade substrates.

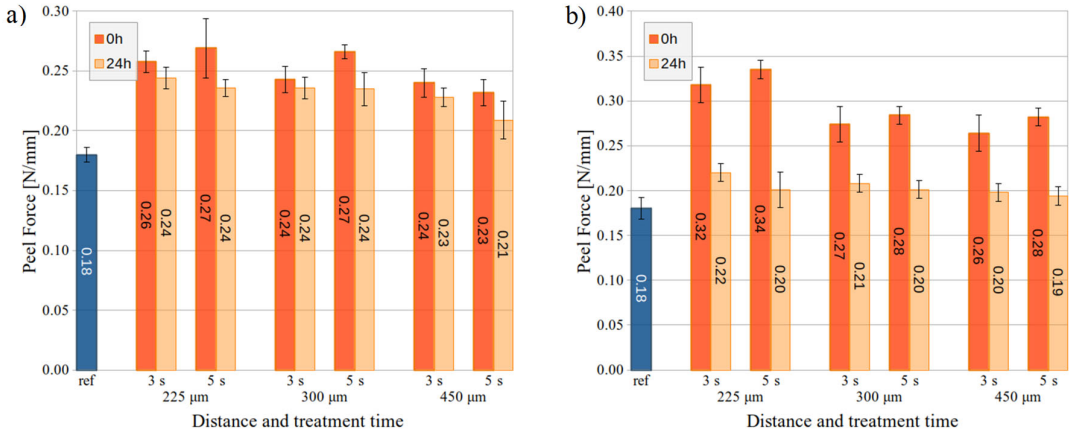

Figure 5. The peel-force of PMMA substrates treated by a) the DCSBD and b) the HDCSBD plasma technology.

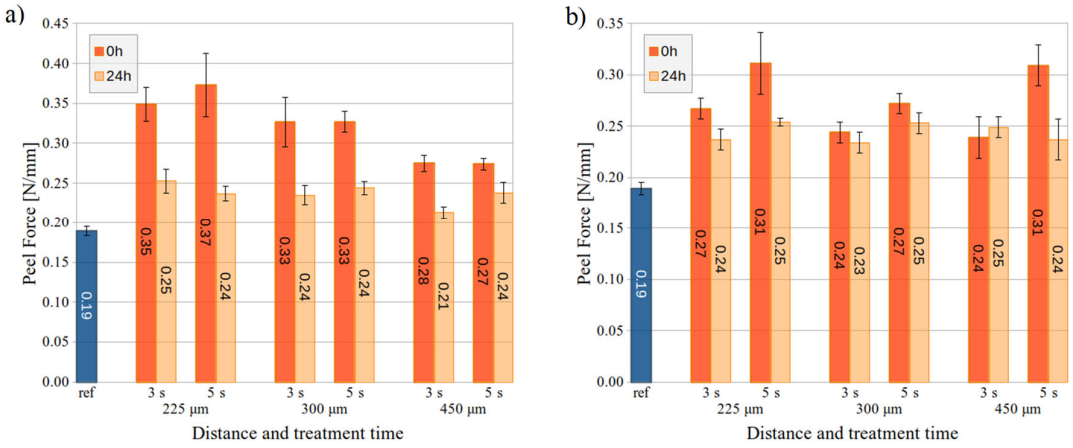

Figure 6. The peel force of PC substrates treated by a) the DCSBD and b) the HDCSBD plasma technology.

After the DCSBD treatment of the PMMA substrate, the adhesion increased, while the 5 s treatment at 225 and 300 um distance showed slightly better performance and peel force 0.27 N/mm. In the case of HDCSBD, higher peel force values (0.26-0.34 N/mm) were achieved after treatment. In this case, prolonged exposure time improved the adhesion, while the distance of the treated substrate had the opposite effect. These tendencies are evaluated within the error. Moreover, it is worth mentioning that lover measurement error (i.e., 5 s treatment) often indicates the improved homogeneity of large surface treatment [10,20,27]. These results correlate also with SFE measurements.

The peel force measurements on the PC substrate showed increased adhesion after the LTP treatment. The substrate adhesion almost doubled in the case of DCSBD at a distance of 225 um. Increasing the distance of the plasma source to the substrate resulted in decreased peel force. The

 doi:10.20944/preprints202402.0178.v1

exception was the 5 s HDCSBD treatment at 450 um, where the surface achieved a comparable peel force of 0.31 N/mm to PC treated at 225 um. In the case of PC, both sources improved surface adhesion performance (average value and/or error ~ homogeneity) after 5 s treatment.

The measuring of PMMA and PC samples stored for 24 hours revealed a dramatic decrease in achieved adhesion, most visible at 225 um distance treatment. Functional groups that aid adhesion at the polymer's substrates include C=O, CO, COO, OH and –OOH. Uptake of environmental contaminants, re-orientation of surface groups and further chemical reactions result in an ageing effect. Therefore, the surface's wettability is recovered with time, thus worsening its adhesion [2,28]. Nevertheless, the studied application of DCSBD and HDCSBD plasma sources in the in/line process should diminish the ageing of pre/treatment.

For further analyses, i.e. XPS, SEM and AFM, the treatment at 225 um distance was excluded due to the high sample amount and data processing time. This decision was supported by the decrease in achieved adhesion after ageing. The decision on further analyses also reflects the studied implementation of plasma pre-treatment into the UV-printing in-line process. Whereas the thickness of industrial-grade transparent polymer substrate can vary on large area plates, the consequential damage (scratching, etc.) could result in the defect of a final product.

3.2. Chemical Changes on LTP-Treated Substrates

The X-ray photoelectron spectroscopy analysis of LTP-treated transparent polymers revealed chemical changes on both substrates. The elemental composition and functional groups concentration on PMMA and PC surfaces before and after plasma treatment are listed in Tab.1 and 2, respectively.

The atomic concentration analysis focused on the main PMMA and PC composing elements, carbon and oxygen, and on nitrogen contained in air. Despite the plasma treatment in air, the atomic concentration of N *1s* increased negligibly after the treatment. The tendencies of increasing concentration due to the time or distance of the treatment are not obvious (within the error). The other element concentrations (e.g. Si *2p*) are not listed in Tables 1 and 2, as they are not expected on pristine samples and implied surface contamination.

Table 1. The atomic concentrations and the relative areas of the C *1s* peak components of the PMMA surface analyzed by XPS measurement after the treatment by HDCSBD.

Treatment [um]		At. Conc. [%][1]				Functional Groups Conc. [%][2]			
		C	O	N	O/C Ratio	C–C/C-H 284.8 eV	C–O 286.7 eV	C–C=O 285.5 eV	O–C=O 288.8 eV
REF	0 s	79	20	-	0.26	52.1	11.7	21.6	14.6
300	3 s	76	22	1.6	0.29	50.9	18.6	18.3	12.2
	5 s	76	19	1.6	0.26	65.2	18.8	7.7	8.3
450	3 s	71	26	2.3	0.36	52.7	24.9	8.6	13.9
	5 s	81	16	1.6	0.20	66.5	16.3	10.1	7.0

[1] Estimated from survey spectra. [2] Estimated by deconvolution of C *1s* high-resolution spectra.[29].

Table 2. The atomic concentrations and the relative areas of C *1s* peak components of the PC surface analyzed by XPS measurement after the treatment by HDCSBD.

Treatment [um]		At. Conc. [%][1]				Functional Groups Conc. [%][2]					
		C	O	N	O/C Ratio	C–C/C-H 284.8 eV	C–O 286.3 eV	C=O 287.8 eV	O–C=O 289.1 eV	O–C=(O)$_2$ 290.6 eV	π–π* 292.2 eV
REF	0 s	88	11	-	0.13	71.4	23.6	-	1.0	3.2	-
300	3 s	74	23	1.8	0.31	65.6	24.3	2.0	6.6	1.6	-
	5 s	76	22	1.5	0.29	65.1	23.4	3.6	4.5	3.1	1.2

 doi:10.20944/preprints202402.0178.v1

450	3 s	81	17	1.0	0.21	73.8	20.3	2.1	3.2	2.0	-
	5 s	77	21	1.3	0.28	65.8	24.1	2.4	3.5	3.5	2.0

[1] Estimated from survey spectra. [2] Estimated by deconvolution of C *1s* high-resolution spectra [30].

After the treatment, the C and O concentration changes are obvious and compared as the O/C ratio. On the PMMA surface, after the 3 s plasma treatment at 300 and 450 um distance, the O/C ratio increased from the initial 0.26 to 0.29 and 0.36, respectively. However, after prolonged treatment (5 s), the O/C ratio reduced to the initial value at 300 μm and decreased even more to 0.20 with increased distance.

The C–C/C-H concentration increase after 5 s treatment indicates cross-linking on the surface induced by prolonged plasma treatment and UV emitted by the plasma [5]. The changes in wettability and surface free energy on PMMA were associated with a pronounced increase in polar components. The C–O group contributing to that component increased after the treatment. The creation of C–O and the loss of other oxygen-containing groups imply their conversion to low-weight volatile fragments (e.g., CO and CO_2) during the LTP interaction [23], contributing to cross-linking.

Similarly to PMMA, the initial O/C ratio on the PC surface (0.13) increased after the plasma treatment by a value of 0.08-0.18. The O/C ratio change was more pronounced for shorter distance. Even though the authors of [31] specified the effective treatment distance to 300 μm, the interaction of surface and plasma also occurs at a higher distance. The UV-resistant PC treated at 450 μm needed more time to increase oxygen concentration to a similar value as in the case of 300 μm. This effect is probably connected to a more remote plasma effect, e.g., gaseous chemical products and long-living particles.

The increase of polar components on the PC surface can be explained by creating polar oxygen-containing functional groups. The deconvolution of C *1s* high-resolution spectra revealed new C=O groups and shake-up-satellites $\pi-\pi^*$. The increase in C=O and O–C=O concentration correlated with the changes in the O/C ratio and mentioned remote plasma effect. These groups contribute profoundly to the polar component of PC SFE. The other oxygen-containing groups decreased after the 3 s plasma treatment but returned to their initial value after the 5 s treatment.

Compared with PMMA, we can assume that cross-linking does not play a role in PC chemical surface changes. Possible hydrogen abstraction from the polymer chain and reduction of nonpolar groups (e.g., methyl) on the surface contributed to C–C/C-H concentration reduction [8,10]. The changes in functional groups are most probably connected with oxygen and nitrogen group incorporation from air and gaseous plasma products. Similar tendencies were observed after air and oxygen plasma treatment [6,32]. The authors of [32] assumed initial sidechain and ring oxidation predominated upon longer plasma treatment.

3.3. Morphological Changes on LTP-Treated Substrates

The polymer-plasma interaction can often cause etching and heat-UV degradation of the surface. However, such effects are not expected after the short LTP treatment. We analyzed the surface roughness and morphological changes using AFM and SEM to confirm the suitability of the plasma and experimental conditions. The roughness values are listed in Tab.3 for pristine and HDCSBD-treated PMMA and PC substrates.

Table 3. The roughness of PMMA and PC after HDCSBD plasma treatment.

PMMA				PC			
Treatment		Roughness [nm]		Treatment		Roughness [nm]	
		RMS	Average			RMS	Average
REF	0 s	3.25	2.58	REF	0 s	0.57	0.31
300 μm	3 s	8.83	6.53	300 μm	3 s	0.52	0.41
	5 s	9.95	7.69		5 s	1.41	0.68
450 μm	3 s	5.49	2.92	450 μm	3 s	0.45	0.37

 doi:10.20944/preprints202402.0178.v1

	PMMA			PC		
	5 s	6.99	4.92	5 s	0.68	0.38

Prolonging the plasma treatment time resulted in an increase in surface roughness on both materials. A similar trend was observed in roughness after shortening the plasma treatment distance. The maximum surface changes were recorded for both substrates after 5 s of plasma exposition at a distance of 300 um.

The roughness values changed more significantly in the case of PMMA. The surface roughness increased approx. 3 and 2 times after treatment at 300 and 450 µm, respectively. In the case of PC, after 5 s treatment, the observed surface roughness increased 2.5 and 1.2 times for the abovementioned distances, respectively.

Following the roughness measurement results, plasma-induced morphological changes are not verifiable from SEM micrographs (Figure 7). After removing the protective tape, dust particles slightly contaminated the substrates due to the created static charge on the substrate. Moreover, the pristine substrates are not perfectly smooth, which suits the AFM results, whereas the pristine PMMA roughness is higher than in the case of PC. The small cracks visible on the micrographs are Au/Pd conductive coating ruptures after the high-energy electron impact at high-resolution mode.

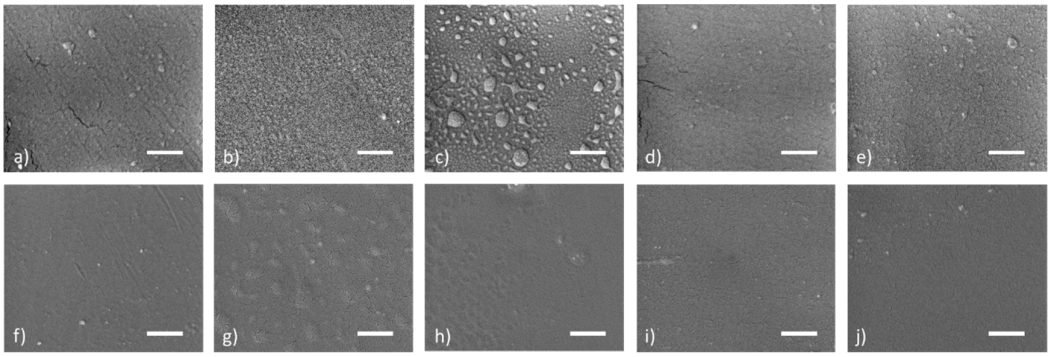

Figure 7. SEM images of PMMA (a-e) and PC (f-j) after different HDCSBD treatment conditions: reference sample (a, f), at 300 um distance treated 3 s (b, g) and 5 s (c, h), at 450 um distance treated 3 s (d, i) and 5 s (e, j) (scale 1 um).

After the LTP plasma treatment at a distance of 300 um, SEM revealed the contamination and roughness changes on the surface of PMMA. The PMMA sample treated 5 s showed visible "bubble-like" structures, implying physicochemical etching of the upper surface, whereas the 3 s treated sample was mostly contaminated with smaller similar structures. After prolonged treatment, we can assume the effect of "bubble" growing by aggregating these smaller structures. Roughness changes are less obvious after treatment at 450 um. Furthermore, the aforementioned structure creation was not apparent from SEM micrographs.

The PC sample LTP treated 3 s and 5s at 300 um distance revealed roughness changes on the part of the surface in comparison to other PC samples. The "swollen" areas were created after 3 s and joined after longer treatment to a larger area. This effect was not visible at a distance of 450 um, and small visible particles indicate contamination from ambient air.

Similarly to the results of chemical characterization, more pronounced changes on both substrates were observed for the LTP treatment at a distance of 300 µm. However, compared to our previous work and works using oxidizing plasma [20,27,30], these changes in roughness and morphology are insignificant, and we did not expect their dominant contribution to ink adhesion. After the LTP treatment, no visible changes were observed in the transparency of the substrates.

 doi:10.20944/preprints202402.0178.v1

3.4. Ink Adhesion of UV-Digital Printing on LTP-Treated Transparent Polymer Substrates

The polymer materials are produced worldwide by different suppliers with slightly different production processes. The end-user of UV digital printers requires a substantial increase in the adhesion of the printed layer and standardization of the printed layer quality. To achieve the best possible results and implementation of an LTP plasma source for flat surface treatment prior to the UV-digital printing, the authors constructed and further optimized the plasma unit introduced in Figure 1b. Due to its robust and compact construction, this HDCSBD was selected as the appropriate plasma source for the in-line UV-printing machine (Figure 2). The optimum conditions for effective large-area UV-digital printing during the in-line testing were set to the distance of 300 um and at treatment times of 1, 3 and 5 s um for both substrates.

The ink hardened by the LED UV lamps is shown in Figures 8–12. The crosscut and tape test qualitatively evaluates the ink-to-substrate bond. All printed patterns presented proper adhesion to the surface of both materials. The differences between untreated and treated surfaces were more visible on dark patterns, consisting of more color pigments (Figure 8.). Thus, we compared the margin of cuts and possible ink shrinkage instead of ISO classification.

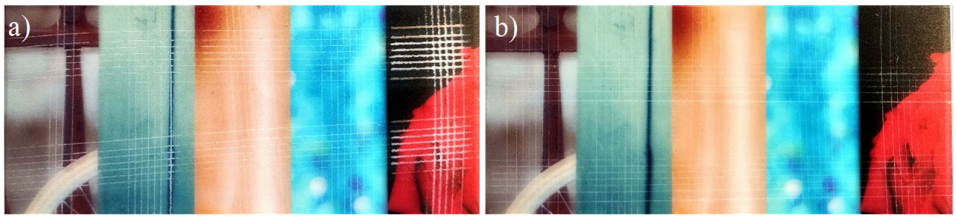

Figure 8. The photographs of colour patterns printed on PMMA substrates after the crosscut test: a) reference and b) 5 s treated.

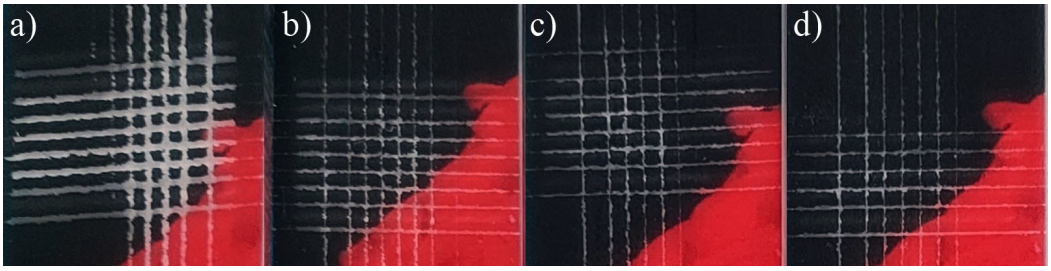

Figure 9. The photograph of the black pattern after the crosscut and tape test right after printing on PMMA substrate treated for a) 0 s, b) 1 s, c) 3 s and d) 5 s.

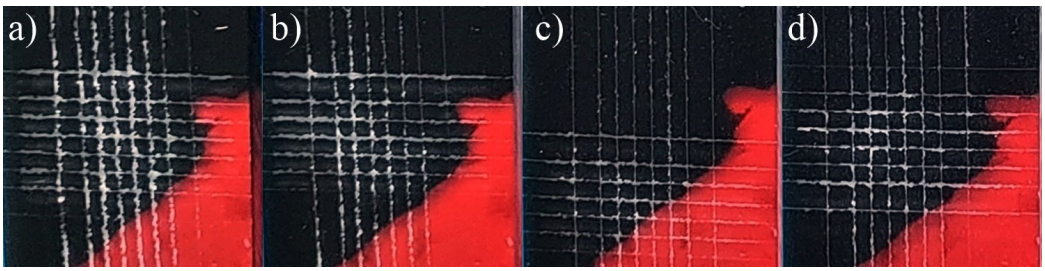

Figure 10. The photograph of the black pattern after the crosscut and tape test after 24 hours of printing on PMMA substrate treated for a) 0 s, b) 1 s, c) 3 s and d) 5 s.

 doi:10.20944/preprints202402.0178.v1

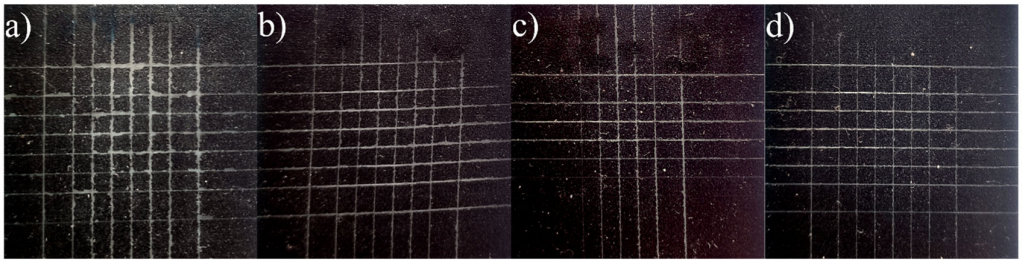

Figure 11. Detail of the black pattern on PC samples after the crosscut and tape test right after the printing: a) reference, treated for b) 1 s, c) 3 s, and d) 5 s.

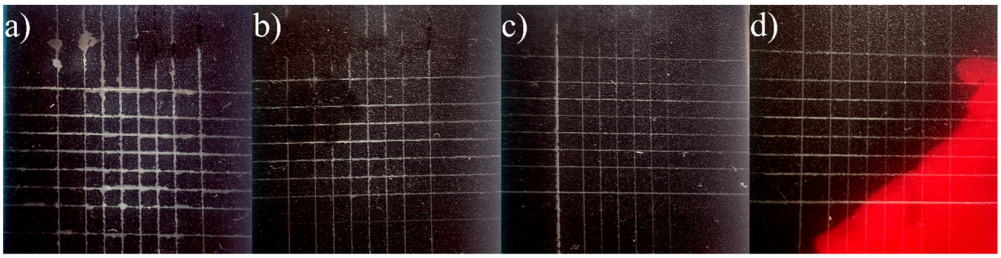

Figure 12. Detail of the black pattern on PC samples after the crosscut and tape test 24 hours after the printing: a) reference, treated for b) 1 s, c) 3 s, and d) 5 s.

After the short plasma treatment of PMMA (Figure 9), the crosscut and tape test revealed a slight improvement in UV-ink adhesion. However, the margin distortion of cut after 24 hours and ink shrinkage (Figure 10) are not substantially reduced on treated PMMA compared to untreated sample. In this case, UV-ink had more time to cure and interact with the LTP-treated substrate. Thus, the cut margins do not show a plain dependence of ink adhesion quality on plasma treatment time.

The change in SFE of the treated surface affects the ink droplet shape and its diameter, which can develop in time. This effect is more pronounced for LTP-treated substrates [16]. Moreover, these authors observed that the UV-ink could undergo considerable degradation of its adhesion after 24 hours on untreated and cleaned surfaces compared to stable ink adhesion to LTP-treated surfaces.

In our case, we did not observe ink adhesion degradation even on untreated PMMA. From the comparison of treated samples cut right after and after 24 hours, we can deduce the ink adhesion improvement due to ink curing and chemical interaction with the functional group created after LTP treatment.

In the case of the PC substrate, the short LTP treatment improved the ink adhesion immediately and 24 hours after printing (Figures 11 and 12). Moreover, the roughness change on the PC surface (chapter 3.3) is not considered dominant in affecting the UV-ink adhesion. The authors link better ink adhesion with SFE increase, adhesion improvement and chemical changes on LTP-treated PC substrate [25,28].

4. Conclusions

This paper introduces a special LTP type for flat PMMA and PC substrate pre-treatment in UV-digital printing applications. The distance range (225-450 um) of the substrate to the plasma source was chosen to fit the requirements of an in-line industrial printing scale. The short (1-5 s) treatment using DCSBD and HDCSBD plasma sources enhanced the surface properties comparably for tested PMMA and PC materials. The activation of substrates was steady within 72 hours, and none of the treated substrates showed full hydrophobic recovery. Since plasma introduced oxygen-containing polar groups onto the surface, SFE increase is ascribed to the polar component. No significant variation is seen for the dispersive component, which agrees with the XPS results. The XPS analyses

revealed the increase of the O/C ratio and implementation of polar functional groups onto both polymer substrates, namely C–O in the case of PMMA and C=O/O–C=O in the case of PC. The morphological changes were minimal within the plasma treatment times and distances used, not affecting the quality and transparency of the material. Minimal morphological changes were observed on SEM micrographs, corresponding with a slight roughness increase on both substrates revealed by AFM.

Even 1 s treatment substantially increased ink adhesion and UV-digital printing quality for PC substrates. For resistant substrates, such as PMMA, longer treatment times were needed. However, improved ink resistance against delamination was achieved on plasma-treated substrates in the vicinity of the cut. According to this study, the authors ascribe the ink adhesion improvement to the chemical changes (SFE, XPS) rather than to the nanoscale roughening of the plasma-treated substrates.

5. Patents

The legally protected outcome and certified technology resulting from the work reported in this manuscript are the Czech utility model "A device for plasma modification of large-area planar substrate before UV-digital printing" (no.2022-39679 pending) and certified technology "Technology for ink adhesion improvement of large-area printing on glass and polymer substrates by atmospheric pressure plasma activation" (soon available at https://www.isvavai.cz/riv).

Author Contributions: Conceptualization, Z.K.T., O.G. and J.K.; methodology, Z.K.T., O.G. and J.K.; validation, M.F., Z.K.T., O.G., E.B. and J.K.; formal analysis, M.F., Z.K.T., O.G., E.B. and T.K.; investigation, Z.K.T. O.G., and J.K.; data curation, M.F., Z.K.T., O.G., E.B. and T.P.; writing—original draft preparation, Z.K.T.; M.F. and O.G., writing—review and editing, X.X.; visualization, M.F., Z.K.T., O.G., E.B.; supervision, Z.K.T. O.G., and J.K.; project administration, D.K. and J.K.; funding acquisition, D.K. and J.K. All authors have read and agreed to the published version of the manuscript.

Funding: This research was funded by the Ministry of Industry and Trade of the Czech Republic under the program TRIO, grant number FV40114, and co-funded by the Ministry of Education, Youth and Sports of the Czech Republic, under the program Large Infrastructures for Research, Development and Innovation, grant numbers LM2018097 and LM2023039.

Data Availability Statement: Not applicable

Acknowledgments: The authors thank project (FV40114) industrial partner Effetec s.r.o. (Čelechovice na Hané, Czech Republic), namely to Lukáš Obšel, Donna Frantík and Zdeněk Přaslička, for providing the support, substrates, and UV-digital printing. The authors thank Jaromír Hašana from Masaryk University for technical support. The authors acknowledge CzechNanoLab Research Infrastructure supported by MEYS CR (LM2018110) for XPS measurement and access to AFM equipment.

This article is dedicated to the memory of our excellent colleague and former principal investigator of project FV40114 at Masaryk University, Dr. Miroslav Zemánek, who passed away in November 2021.

Conflicts of Interest: The authors declare no conflict of interest.

References

1. Kogelschatz, U. Dielectric-barrier Discharges : Their History , Discharge Physics , and Industrial Applications. *Plasma Chem. Plasma Process.* **2003**, *23*, 1–46.
2. Kusano, Y. Atmospheric pressure plasma processing for polymer adhesion: A review. *J. Adhes.* **2014**, *90*, 755–777, doi:10.1080/00218464.2013.804407.
3. Nemani, S.K.; Annavarapu, R.K.; Mohammadian, B.; Raiyan, A.; Heil, J.; Haque, M.A.; Abdelaal, A.; Sojoudi, H. Surface Modification of Polymers: Methods and Applications. *Adv. Mater. Interfaces* **2018**, *5*, 1801247, doi:10.1002/ADMI.201801247.
4. Brès, L.; Sanchot, A.; Rives, B.; Gherardi, N.; Naudé, N.; Aufray, M. Fine-tuning of chemical and physical polymer surface modifications by atmospheric pressure post-discharge plasma and its correlation with adhesion improvement. *Surf. Coatings Technol.* **2019**, *362*, 388–396, doi:10.1016/J.SURFCOAT.2019.01.102.
5. Wertheimer, M.R.; Fozza, A.C.; Holländer, A. Industrial processing of polymers by low-pressure plasmas: the role of VUV radiation. *Nucl. Instruments Methods Phys. Res. Sect. B Beam Interact. with Mater. Atoms* **1999**, *151*, 65–75, doi:10.1016/S0168-583X(99)00073-7.

6. Gizer, S.G.; Bhethanabotla, V.R.; Ayyala, R.S.; Sahiner, N. Low-pressure plasma treated polycarbonate and polymethyl methacrylate (PMMA) sheets with different surface patterns to change their surface properties. *Surfaces and Interfaces* **2023**, *37*, 102646, doi:10.1016/j.surfin.2023.102646.
7. Moraczewski, K.; Rytlewski, P.; Malinowski, R.; Zenkiewicz, M. Comparison of some effects of modification of a polylactide surface layer by chemical, plasma, and laser methods. *Appl. Surf. Sci.* **2015**, *346*, 11–17, doi:10.1016/j.apsusc.2015.03.202.
8. Dorai, R.; Kushner, M.J. A model for plasma modification of polypropylene using atmospheric pressure discharges. *J. Phys. D. Appl. Phys.* **2003**, *36*, 666–685, doi:10.1088/0022-3727/36/6/309.
9. Černák, M.; Černáková, L.; Hudec, I.; Kováčik, D.; Zahoranová, A. Diffuse Coplanar Surface Barrier Discharge and its applications for in-line processing of low-added-value materials. *Eur. Phys. J. Appl. Phys.* **2009**, *47*, 22806, doi:10.1051/epjap/2009131.
10. Šrámková, P.; Tučeková, Z.K.; Fleischer, M.; Kelar, J.; Kováčik, D. Changes in surface characteristics of BOPP foil after treatment by ambient air plasma generated by coplanar and volume dielectric barrier discharge. *Polymers (Basel).* **2021**, *13*, 12, doi:10.3390/POLYM13234173.
11. Štěpánová, V.; Šrámková, P.; Sihelník, S.; Stupavská, M.; Jurmanová, J.; Kováčik, D. The effect of ambient air plasma generated by coplanar and volume dielectric barrier discharge on the surface characteristics of polyamide foils. *Vacuum* **2021**, *183*, 109887, doi:10.1016/j.vacuum.2020.109887.
12. Zhang, C.; Zhao, M.; Wang, L.; Yu, M. Effect of atmospheric-pressure air/He plasma on the surface properties related to ink-jet printing polyester fabric. *Vacuum* **2017**, *137*, 42–48, doi:10.1016/J.VACUUM.2016.12.029.
13. Sandanuwan, T.; Hendeniya, N.; Attygalle, D.; Amarasinghe, D.A.S.; Weragoda, S.C.; Samarasekara, A.M.P.B. Atmospheric cold plasma to improve printability of polyethylene terephthalate. *MERCon 2021 - 7th Int. Multidiscip. Moratuwa Eng. Res. Conf. Proc.* **2021**, 654–658, doi:10.1109/MERCon52712.2021.9525797.
14. Pawlak, D.; Boruszewski, P. Digital printing in wood industry. *Ann. Warsaw Univ. Life Sci. For. Wood Technol.* **2020**, *109*.
15. Wan, H.; Song, D.; Li, X.; Zhang, D.; Gao, J.; Du, C. Failure Mechanisms of the Coating/Metal Interface in Waterborne Coatings: The Effect of Bonding. *Materials (Basel).* **2017**, *10*, 397, doi:10.3390/MA10040397.
16. Tofan, T.; Jasevičius, R. Modelling of the motion and interaction of a droplet of an inkjet printing process with physically treated polymers substrates. *Appl. Sci.* **2021**, *11*, doi:10.3390/app112311465.
17. Stepanova, V.; Kelar, J.; Galmiz, O.; Zemanek, M.; Slavicek, P.; Bucek, A.; Cernak, M. Areal homogeneity verification of plasma generated by diffuse coplanar surface barrier discharge in ambient air at atmospheric pressure. *Contrib. to Plasma Phys.* **2017**, *57*, 182–189, doi:10.1002/ctpp.201600093.
18. Owens, D.K.; Wendt, R.C. Estimation of the surface free energy of polymers. *J. Appl. Polym. Sci.* **1969**, *13*, 1741–1747, doi:10.1002/app.1969.070130815.
19. Homola, T.; Matoušek, J.; Hergelová, B.; Kormunda, M.; Wu, L.Y.L.; Černák, M. Activation of poly (methyl methacrylate) surfaces by atmospheric pressure plasma. *Polym. Degrad. Stab.* **2012**, *97*, 886–892, doi:10.1016/j.polymdegradstab.2012.03.029.
20. Kelar, J.; Shekargoftar, M.; Krumpolec, R.; Homola, T. Activation of polycarbonate (PC) surfaces by atmospheric pressure plasma in ambient air. *Polym. Test.* **2018**, *67*, 428–434, doi:10.1016/J.POLYMERTESTING.2018.03.027.
21. Encinas, N.; Díaz-Benito, B.; Abenojar, J.; Martínez, M.A. Extreme durability of wettability changes on polyolefin surfaces by atmospheric pressure plasma torch. *Surf. Coatings Technol.* **2010**, *205*, 396–402, doi:10.1016/j.surfcoat.2010.06.069.
22. Lapena, M.H.; Lopes, C.M.A. Improvement of aerospace thermoplastic composite adhesion to coating with dielectric barrier discharge atmospheric pressure plasma surface treatment. *Plasma Process. Polym.* **2023**, *20*, doi:10.1002/ppap.202200081.
23. Abdel-Fattah, E. Surface Activation of Poly(Methyl Methacrylate) with Atmospheric Pressure Ar + H 2 O Plasma. **2019**, doi:10.3390/coatings9040228.
24. Suzer, S.; Argun, A.; Vatansever, O.; Aral, O. *XPS and Water Contact Angle Measurements on Aged and Corona-Treated PP*; 1999; Vol. 74;.
25. Baldan, A. Adhesion phenomena in bonded joints. *Int. J. Adhes. Adhes.* **2012**, *38*, 95–116, doi:10.1016/j.ijadhadh.2012.04.007.
26. Hitchcock, S.J.; Carroll, N.T.; Nicholas, M.G. Some effects of substrate roughness on wettability. *J. Mater. Sci. 1981 163* **1981**, *16*, 714–732, doi:10.1007/BF02402789.
27. Shekargoftar, M.; Kelar, J.; Krumpolec, R.; Jurmanova, J.; Homola, T. A Comparison of the Effects of Ambient Air Plasma Generated by Volume and by Coplanar DBDs on the Surfaces of PP/Al/PET Laminated Foil. *IEEE Trans. Plasma Sci.* **2018**, *46*, 3653–3661, doi:10.1109/TPS.2018.2861085.
28. Awaja, F.; Gilbert, M.; Kelly, G.; Fox, B.; Pigram, P.J. Adhesion of polymers. *Prog. Polym. Sci.* **2009**, *34*, 948–968, doi:10.1016/J.PROGPOLYMSCI.2009.04.007.

29. Pletincx, S.; Marcoen, K.; Trotochaud, L.; Fockaert, L.L.; Mol, J.M.C.; Head, A.R.; Karslioğlu, O.; Bluhm, H.; Terryn, H.; Hauffman, T. Unravelling the Chemical Influence of Water on the PMMA/Aluminum Oxide Hybrid Interface In Situ. *Sci. Reports 2017 71* **2017**, *7*, 1–11, doi:10.1038/s41598-017-13549-z.
30. Tompkins, B.D.; Dennison, J.M.; Fisher, E.R. Etching and Post-Treatment Surface Stability of Track-Etched Polycarbonate Membranes by Plasma Processing Using Various Related Oxidizing Plasma Systems. *Plasma Process. Polym.* **2014**, *11*, 850–863, doi:10.1002/PPAP.201400044.
31. Šimor, M.; Ráhel', J.; Vojtek, P.; Černák, M.; Brablec, A. Atmospheric-pressure diffuse coplanar surface discharge for surface treatments. *Appl. Phys. Lett.* **2002**, *81*, 2716–2718, doi:10.1063/1.1513185.
32. Muir, B.W.; Mc Arthur, S.L.; Thissen, H.; Simon, G.P.; Griesser, H.J.; Castner, D.G. Effects of oxygen plasma treatment on the surface of bisphenol A polycarbonate: a study using SIMS, principal component analysis, ellipsometry, XPS and AFM nanoindentation. *Surf. Interface Anal.* **2006**, *38*, 1186–1197, doi:10.1002/SIA.2363.